Orissa Journal of Physics
ISSN 0974-8202

Vol. 25, No.1
February 2018
pp. 63-69

The Interplay of the Coulomb potential and transverse gate potential in Anti-ferromagnetic Order in AA-Stacked Bi-layer Graphene: A Tight Binding Study

R SWAIN[1], S SAHU[2]and G C ROUT[3]

[1]*School of Applied Sciences (Physics), KIIT University, Bhubaneswar, Pin-751024*
[2]*School of Basic Sciences, Indian Institute of Technology, Bhubaneswar-751007*
[3]*Condensed Matter Physics Group ,Physics Enclave, PlotNo.- 664/4825, Lane -4A,Shree Vihar, Patia, Bhubaneswar- 751031, Odisha,India*
**Corresponding author- gcr@iopb.res.in*

Received: 13.11.2017 ; Revised : 18.12.2017 ; Accepted : 11.1.2018

Abstract. In order to describe the anti-ferromagnetic spin ordering in AA-stacked bi-layer graphene, we have proposed a tight- binding model Hamiltonian consisting of nearest-neighbor $2P_z$ electron hopping of carbon atom and the interlayer electron hopping. The on-site Coulomb potential introduces the anti-ferromagnetic order in the system. We have assumed that the spin ordering of one carbon atom in a layer is opposite to that of the neighboring carbon atoms. We have introduced a transverse gate potential which can tune the anti-ferromagnetic order in the system. The Hamiltonian is solved by Zubarev's Green's function technique. Finally the temperature dependent anti-ferromagnetic gap is derived from the correlation functions obtained from the Green's functions and consequently the results are discussed.

Keywords: Graphene, Anti-ferromagnetism, AA-stacked bi-layer graphene

1. Introduction

Pristine single layer graphene has no gap in electronic spectrum near Dirac point [1, 2]. Bi-layer graphene consists of two hexagonal layers with new unusual physical properties and spectrum, which are different from the single layer graphene, in which AA-stacked and AB-stacked bi-layer graphene can be formed. Now a days mono-layer graphene and bi-layer graphene (BLG) are also interesting research areas to prepare graphene based materials with a tunable gap. More recently experimental realization of AA and AB-stacked graphene has been reported [3, 4]. In AA-stacked BLG, the A sub-lattice of the top layer is stacked directly above the same sub-lattice of the bottom layer. The energy band of AA-stacked BLG consists of four energy bands of which two are conduction bands and two are valance bands which. The bands are shifted up and down by the interlayer coupling γ=0.2eV. The most important character of AA-BLG is that the conduction and valence band coincide in the un-doped material [5]. These degenerate Fermi surfaces are unstable, when an arbitrary weak electron interaction is present and bi-layer system becomes an anti-ferromagnetic (AFM) insulator with a finite gap. This electronic instability is the strongest, when the bands cross at the Fermi level. The on-site Coulomb repulsion is the strongest interaction in AA-stacked BLG system and this interaction is sufficient for stability or meta-stability of the AFM order. Here we investigate the evolution of the anti-ferromagnetic order in AA-stacked BLG by using tight binding Hamiltonian model with interlayer and interlayer electron hoppings, transverse electric field and Coulomb interaction.

2. Model Hamiltonian

The monolayer graphene has honey-comb lattice with A and B sub-lattices. The bi-layer graphene (BLG) consists of two monolayers with AA-stacked AB-stacked BLG systems. Here A_1 and B_1 are the two sub-lattice atoms in first layer, while A_2 and B_2 are in second layer. Two similar sub-lattice atoms lie one above the other in AA-stacked BLG. The unit cell of AA-stacked BLG contains four atoms like A_1, B_1, A_2 and B_2. Anti-ferromagnetism develops in AA-stacked BLG, where the spin of a particular atom is opposite in direction to the surrounding atoms. Hence the single particle Hamiltonian for AA-stacked bi-layer graphene is given by

$$H_1 = \sum_{\alpha,k,\sigma} \left(\mu + xU_0 - (-1)^{\alpha}(\frac{V}{2} + \Delta_A)\right) a^{\dagger}_{\alpha,k,\sigma} a_{\alpha,k,\sigma} + \sum_{\alpha,k,\sigma} \left(\mu - (-1)^{\alpha}(\frac{V}{2} - \Delta_A)\right) b^{\dagger}_{\alpha,k,\sigma} b_{\alpha,k,\sigma} \quad (1)$$

The Hamiltonian H_1 represents on-site electron hopping and here $a^{\dagger}_{\alpha,k,\sigma}$ $(a_{\alpha,k,\sigma})$and $b^{\dagger}_{\alpha,k,\sigma}$ $(b_{\alpha,k,\sigma})$are the creation (annihilation) operators of electrons with spin σ in the layers $\alpha = 1\,, 2$ on the sub-lattices A and B. μ,x and U_0 represent respectively the chemical potential, doping concentration and impurity potential at A-sites of both the layers. A transverse gate potential (V) is applied between two layers with $V \ll t_1$ [6, 7]. The anti-ferromagnetic gap Δ_A develops in AA-stacked BLG.

$$H_2 = \sum_{<\alpha,k,\sigma>} (\epsilon_k\, a^{\dagger}_{\alpha,k,\sigma}\, b_{\alpha,k,\sigma} + \epsilon^*_k b^{\dagger}_{\alpha,k,\sigma} a_{\alpha,k,\sigma}) \quad (2)$$

The Hamiltonian H_2 in equation (2) represents the hopping of electrons to nearest-neighbor lattice points having hopping energy $\epsilon_k = t_1\gamma_1(k)$ with $t_1 = 2.78$ eV with nearest-neighbor in-plane hopping integral and $\gamma_1(k)$ is the nearest-neighbor electron dispersion.

$$H_{AA} = \sum_{\alpha,\beta,k,\sigma} [\,\epsilon_{k,\perp} a^{\dagger}_{\alpha,k,\sigma} a_{\beta,k,\sigma} + \epsilon^{*}_{k,\perp} b^{\dagger}_{\alpha,k,\sigma} b_{\beta,k,\sigma} + \mathrm{h.c.}\,]$$

$$\alpha, \beta = 1\,, 2 \;\; \& \;\; \alpha \neq \beta \tag{3}$$

The Hamiltonian H_{AA} represents the hopping of electrons from first layer to second layer for vice-versa with inter plane hopping energy $\epsilon_{k,\perp} = t_{\perp}|\gamma_{\perp}(k)|$. Here $t_{\perp} = 0.4$ and $|\gamma_{\perp}(k)|$ are the perpendicular hopping integral and interlayer dispersion. The total Hamiltonian is given by $H = H_1 + H_2 + H_{AA}$

3. Calculation of Green's functions and AFM gap equation for AA-BLG

We calculate the four coupled electron Green's functions involving electrons of A site as well as B site carbon atoms and they are written as

$$A_{\alpha,\beta}(k,\omega) = \ll a_{\alpha,k,\sigma}\;; a^{\dagger}_{\beta,k,\sigma} \gg_{\omega} \;;\; B_{\alpha,\beta}(k,\omega) = \ll b_{\alpha,k,\sigma}\;; b^{\dagger}_{\beta,k,\sigma} \gg_{\omega} \tag{4}$$

where $\alpha = 1,2$ for two layers and $\beta = 1-4$ for four Green's functions. The coupled Green's functions are calculated by Zubarev's techniques [8] and for first layer at A site and B sites these are written as $A_{1,1}(k,\omega) = \frac{p_{22}}{2\pi|D(\omega)|}$; $B_{1,1}(k,\omega) = \frac{q_{22}}{2\pi|D(\omega)|}$,where p_{22} and q_{22} are not give explicitly. The denominator terms $|D(\omega)|$in the above expression can be written as$|D(\omega)| = |D_1(\omega)||D_2(\omega)| - \left[\left(\overline{\omega}^2 - V^{+2}\right) + \left(\overline{\omega}^2 - V^{-2}\right)\right]|\epsilon_{k\perp}|^2 - 2\,|\epsilon_k|^2|\epsilon_{k\perp}|^2 + |\epsilon_{k\perp}|^4$,
where$|D_1(\omega)| = (\varpi - V^+)(\varpi - V^-) - |\epsilon_k|^2$&$|D_2(\omega)| = (\varpi + V^+)(\varpi + V^-) - |\epsilon_k|^2$,$\varpi = \omega - \mu$, $V^+ = \frac{V}{2} + \Delta_A$ and $V^- = \frac{V}{2} - \Delta_A$. Equating the $|D(\omega)|$ to zero i.e. $|D(\omega)| = 0$, we get the quasi-particle dispersion energies $\omega_{\alpha,s}(k)$ which are given below

$$\omega_{\alpha,s}(k) = \mu - (-1)^s\sqrt{A_k - 2(-1)^{\alpha} B_k}\;\; , \alpha \;\&\; s = 1,2 \tag{5}$$

where $A_k = \frac{V^2}{4} + \Delta_A^2 + |\epsilon_k|^2 + |\epsilon_{k\perp}|^2$; $B_k = \sqrt{\frac{V^2}{4}\Delta_A^2 + |\epsilon_k|^2\left(\,|\epsilon_{k\perp}|^2 + \frac{V^2}{4}\right)}$

The AFM gap equation is written as

$$\Delta_A = \frac{S}{(2\pi)^2}\iint dk_x dk_y\left[\left(<n_{1,\downarrow}^{b}> - <n_{1,\uparrow}^{a}>\right) - \left(<n_{2,\uparrow}^{b}> - <n_{2,\downarrow}^{a}>\right)\right] \quad (6)$$

Where $<n_{\alpha,\sigma}^{\gamma}>$ represents the electron densities at different sites $\gamma = A, B$, both layers ($\alpha = 1,2$) for both spins ($\sigma = \uparrow, \downarrow$). All the parameters appearing in the calculation are scaled by nearest-neighbor hopping integral t_1. The dimensionless quantities are written as: The site energy at A site ea = $\frac{\epsilon_a}{t_1}$, site energy at B site eb = $\frac{\epsilon_b}{t_1}$, gate potential v = $\frac{V}{t_1}$, nearest- neighbor hopping integral $\tilde{t}_1 = -1$, AFM gap $z = \frac{\Delta_A}{t_1}$ and Coulomb energy $u = \frac{U}{t_1}$.

4. Results and Discussion

The anti-ferromagnetic(AFM) gap equation given in equation (6) is solved self- consistentily for different values of transverse gate potentials, $\boldsymbol{v = 0.035 - 0.044}$ as shown in figure 1. For a given gate potential $\boldsymbol{v = 0.035}$, the AFM gap starts from the value $\boldsymbol{z = 0}$ at temperature $\boldsymbol{t \approx 0.15}$, then increases to attain a flat maximum at temperature $\boldsymbol{t \approx 0.8}$, then decreases at higher temperatures upto Neel temperature, $\boldsymbol{t_N \approx 1.18}$. Thus the AMF gap exhibits mean field behavior at its second part. However the AFM gap exhibits a large supression at low temperature showing re-entrant behavior. When higher transverse gate potentials are applied, the AFM gap is enhanced throughout the temperature range associated with the enhancement of the Neel temperature . In addition the re-entrant behavor in anti-ferromagnetic order at low temperatures vanishes as shown by the existance of a finite anti-ferromagnetic order.

The figure 2 shows the interplay of Coulomb potential ($\boldsymbol{u}$) and transverse gate potential ($\boldsymbol{v}$) on the AFM gap for different values of different gate potentials, $\boldsymbol{v = 0.035 - 0.044}$. For a given lower gate potential, $\boldsymbol{v = 0.035}$ the anti-ferromagnetic order is absent for the Coulomb potential $\boldsymbol{u < 0.855}$. The AFM gap gradually increases with increase of Coulomb potential to achive its maximum value, $\boldsymbol{z_{max} \approx 7.0}$ corresponding to the Coulomb potential $\boldsymbol{u \approx 2.0 (U = u \times t_1 \approx 2.0 \times 2.78 eV \approx 5.56\, eV)}$. The AFM gap shows a small sharp drop at $\boldsymbol{u = 2.0}$, then remains constant for $\boldsymbol{u > 2.0}$, indicating that the magnitude of the AFM order remains constant. It is to mention here that for a given Coulomb potential, the AFM gap is enhanced with increase of the transverse gate potential. Simultaneously the position of the AFM gap maximum shifts to lower Coulomb potential with increase of the gate potential and shifts to higher Coulomb potential with decrease of gate potential. It is mention worthy that the gate potential decrease the minimum Coulomb potential with a very small amount. Thus the Coulomb potential and gate potential display an interesting interplay in the anti-ferromagnetic order in AA-stacked bi-layer graphene(BLG).

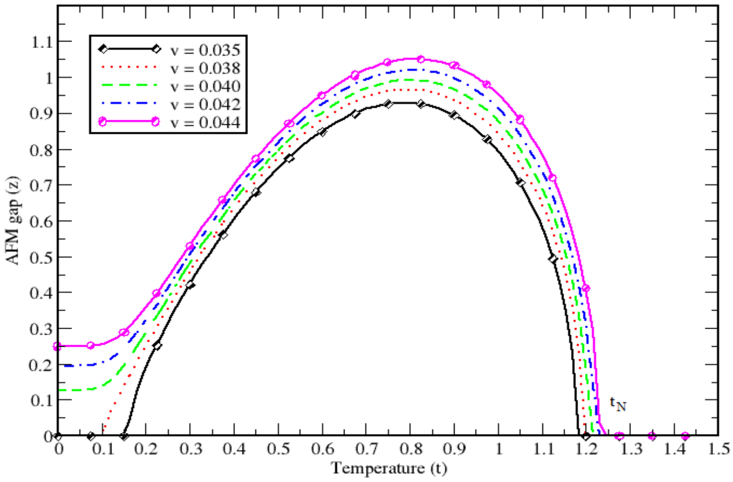

Figure 1. Plot of AFM gap (z) vs. temperature (t) for different Gate potentials v = 0.035 − 0.044 at fixed Coulomb energy u = 0.855 and interlayer hopping energy $\boldsymbol{tp = 0.143}$

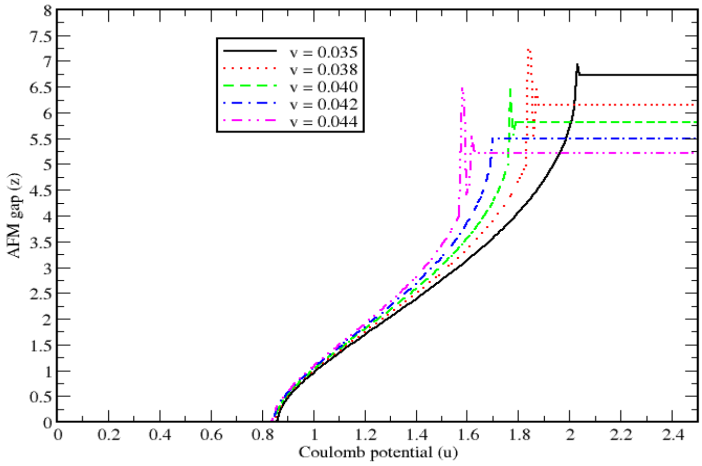

Figure 2. Plot of AFM gap (z) vs. Coulomb potential (u) for different gate potential v = 0.035 − 0.044 at a fixed temperature t = 0.01 and interlayer hopping energy $\boldsymbol{tp = 0.143}$

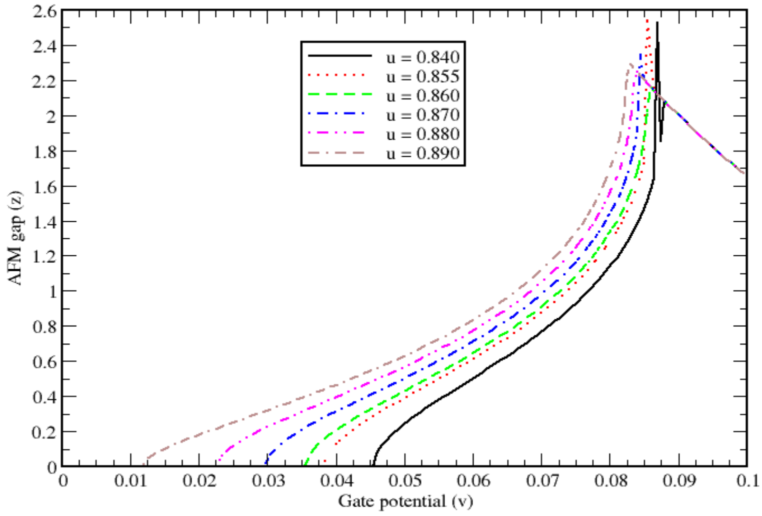

Figure 3. Plot of AFM gap (z) vs. Gate potential (v) for different Coulomb potential u = 0.840 − 0.890 at a fixed temperature t = 0.01 and interlayer hopping energy $\boldsymbol{tp = 0.143}$

The figure 3 shows the effect of Coulomb potential on AFM gap as a function of gate potential. For a given lower Coulomb potential $\boldsymbol{u = 0.840}$, the anti-ferromagnetic order is completely absent for the gate potential $\boldsymbol{v \approx 0.045 (V \approx 0.045 \times t_1 = 0.045 \times 2.78eV \approx 0.1251eV)}$. The AFM gap starts from zero at $\boldsymbol{v = 0.045}$ for $\boldsymbol{u = 0.840,}$ then increases with increase of gate potential to attain its peak value, $\boldsymbol{z_{max} \approx 2.5}$ for gate potential $\boldsymbol{v = 0.0875}$ ($\boldsymbol{V \approx 0.0875 \times 2.78eV = 0.243eV}$) and then reduces sharply for higher values of gate potentials. This indicates that A-site magnetization is greater for the gate potential lying in the range $\boldsymbol{0.045 - 0.0875}$ and the B-site magnetization gradually becomes higher compared to A-site magnetization for the gate potential $\boldsymbol{v > 0.0875}$. At a given finite gate potential, the AFM gap is enhanced with increase of the Coulomb potential. It is to mention here that, with increase of Coulomb potential, a lower magnitude of gate potential can induce anti-ferromagnetic order in the AA-stacked BLG. With increse of the Coulomb potential from $\boldsymbol{u = 0.840}$ to $\boldsymbol{u = 0.890}$ the minimum gate potential to induce anti-ferromagnetic order in AA-stacked BLG reduces from $\boldsymbol{v \approx 0.045}$ to $\boldsymbol{v \approx 0.0125}$. This study again clearly exhibits the interesting interplay between Coulomb potential and transverse gate potential in inducing the AFM order in the system.

5. Conclusions

We have proposed a tight-binding model study for the temperature dependent anti-ferromagnetic magnetization in AA-stacked BLG by introducing on-site repulsive Coulomb potential and transverse gate potential. All the calculations are carried out by Zubarev's Green's function technique. This work presents an interesting interplay of Coulomb potential and gate potential for the on-set of anti-ferromagnetic order in AA-stacked BLG.

References

[1] AH Castro Neto, F Guinea, KS Novoselov et al., *Rev. Mod. Phys*. **81**, 109 (2009)

[2] DSL Abergel, V Apalkov, J Berashevich, K Ziegler, and T Chakraborty, *Adv. Phys*. **59**, 261 (2010)

[3] Z Liu, K Suenaga, P J F Harris and S Iijima , *Phys. Rev. Lett*. **102**,015501 (2009)

[4] J Borysiuk , J Soltys and J Piechota, *J. Appl. Phys*. **109**, 093523 (2011)

[5] AL Rakhmanov, AV Rozhkov, AO Sboychakov et.al., *Phys Rev. Lett*. **109**, 206801(2012)

[6] EV Castro, KS Novoselov. SV Morozov, N M Peres et.al. *Phys. Rev. Lett*. **99** , 216802 (2007)

[7] Y Zhang, T-T Tang , C Girit, Z Hao et.al. *Nature* (London) **459**, 820 (2009)

[8] D N Zubarev, *Sov. Phys. Usp*. **3**, 320 (1960)